ten times that of the two cadmium isotopes. However, the observed level spacings are 68 for Cd^{111}, 61 for Cd^{113}, and 14 for In^{113}.[10] This contradiction by a direct measurement of the level spacing has been discussed previously[11,12] and appears to be quite general for many isotopes.

The resonance absorption integral calculated from the B-W resonance parameters above 0.4 ev is 17.5 ± 3.0 barns. Known resonances up to 215 ev contribute 12.7 barns to the resonance integral. Above this energy average parameters were used to estimate the remaining 5.2 barns. An absorption integral of this magnitude is expected to have little effect on thermal reactor neutron economy when cadmium is used as control rods. As a filter for fast neutron spectrometers, cadmium must be used with caution since neutrons at the resonance energies will be depleted.

[10] Harvey, Hughes, Carter, and Pilcher, Phys. Rev. **99**, 10 (1955).
[11] H. Hurwitz, Jr., and H. A. Bethe, Phys. Rev. **81**, 898 (1951).
[12] Harris, Muehlhause, and Thomas, Phys. Rev. **79**, 11 (1950).

V. ACKNOWLEDGMENTS

The authors wish to acknowledge the assistance of Barbara Brown in the processing of the data, and Loel McClellan for his help with the operation of the chopper.

PHYSICAL REVIEW VOLUME 105, NUMBER 2 JANUARY 15, 1957

Bremsstrahlung Measurements with a Compton Electron Spectrometer*†

J. W. Robson‡ and E. C. Gregg
Case Institute of Technology, Cleveland, Ohio

(Received September 19, 1955; revised version received October 11, 1956)

A method of analyzing the data obtained from a Compton electron spectrometer in order to obtain the incident photon spectrum is described. Practical considerations limit the application of this analysis to photon energies above about 5 Mev. Application of this analysis to a measurement of the spectrum of the Case betatron is described.

I. INTRODUCTION

A NUMBER of techniques have been applied to the analysis of a continuous photon spectrum.[1–8] In this paper we will describe the use of a Compton electron spectrometer in measuring the spectrum of the Case flux-forced field-biased betatron.[9] The principle difference between the work reported here and that done by the group at the National Bureau of Standards[6–8] is in the method employed to obtain the incident photon spectrum from the measured spectrum of Compton electrons.

The operation of the Compton spectrometer depends upon a measurement of the energy spectrum of the Compton electrons which are ejected from a metallic scatterer at a given angle from the photon beam being studied. By considering the Compton energy-angle relations, the Klein-Nishina cross section, and the scattering and energy loss of the electrons in the scatterer, we can relate the kinetic energy spectrum of the detected electrons to the incident photon spectrum. Of the interactions between the incident photons and the electrons and nuclei of the scatterer, only those resulting in electrons leaving the scatterer are of interest and we can thus limit our attention to the photoelectric effect, the Compton effect, and pair production. In order to use the Compton energy-angle relations, we must minimize or make corrections for electrons from the other two interactions. Since the probability of a Compton interaction relative to the other two increases with decreasing atomic number, we chose beryllium as a scattering material. In the energy range of this instrument the photoelectric effect in beryllium is completely negligible and pair production may be expected to contribute no more than 20% of the observed electrons. If we assume that the electrons and positrons from pair production have the same angular distribution, we can measure the positrons and make a correction for the pair electrons. The Compton electrons lose energy and are multiply scattered through Coulomb interactions in the scatterer, and thus the simple Compton energy-angle relations are not sufficient to relate the energy of an electron leaving the scatterer in a known direction to the energy of the photon which ejected it. Fortunately, the energy loss in the energy

* This work was supported by the U. S. Atomic Energy Commission.
† From a thesis submitted by one of the authors (J. W. R.) to Case Institute of Technology in partial fulfillment of the requirements for the degree of Doctor of Philosophy.
‡ Present address: University of Arizona, Tucson, Arizona.
[1] W. Bosley *et al.*, Nature **161**, 1022 (1948).
[2] H. W. Koch and R. E. Carter, Phys. Rev. **75**, 1950 (1949).
[3] R. M. Warner and E. F. Shrader, Rev. Sci. Instr. **25**, 663 (1954).
[4] V. E. Krohn and E. F. Shrader, Phys. Rev. **86**, 391 (1952).
[5] W. B. Lasich and L. Riddiford, J. Sci. Instr. **24**, 177 (1947).
[6] J. W. Motz, Phys. Rev. **86**, 753 (1952).
[7] Motz, Miller, and Wyckoff, Phys. Rev. **89**, 968 (1953).
[8] J. W. Motz *et al.*, Rev. Sci. Instr. **24**, 929 (1953).
[9] E. C. Gregg, Rev. Sci. Instr. **22**, 176 (1951).

range of interest is practically independent of the energy of the electron and small enough that we can safely neglect it, and the effect of multiple scattering can be included in a deduction of the response of the spectrometer. It is also fortunate that the choice of a scatterer with a low atomic number minimizes the effect of multiple scattering.

II. SPECTROMETER RESPONSE

A theory relating the observed electron counting rates to the incident photon spectrum will be presented and the actual calculations will be outlined. Consider first the incident photon spectrum. Let the number of photons per unit area per unit time with energy between E_γ and $E_\gamma+dE_\gamma$ be $B(E_\gamma)dE_\gamma$. These photons will interact in the scatterer and produce Compton electrons having various values of kinetic energy, T, directed at various angles, ψ, with respect to the direction of the incident photon beam. The kinetic energy and angle of scattering will be related by

$$T=\frac{2mc^2E_\gamma^2\cos^2\psi}{(mc^2)^2+2mc^2E_\gamma+E_\gamma^2\sin^2\psi}. \tag{1}$$

The number of Compton electrons scattered between ψ and $\psi+d\psi$ by photons having energy between E_γ and $E_\gamma+dE_\gamma$ will be given by

$$U(\psi,E_\gamma)d\psi=N\frac{\partial\sigma}{\partial\psi}B(E_\gamma)dE_\gamma d\psi, \tag{2}$$

where $\partial\sigma/\partial\psi$ is the Klein-Nishina cross section per unit electron angle and N is a constant depending on the exposed area and the electron density of the scatterer. The number of these electrons which will be accepted by the magnetic analyzer will be given by

$$V(\psi,E_\gamma)d\psi=A(\psi,E_\gamma)N\frac{\partial\sigma}{\partial\psi}B(E_\gamma)dE_\gamma d\psi, \tag{3}$$

where $A(\psi,E_\gamma)$ is the probability that a Compton electron initially scattered between ψ and $\psi+d\psi$ by a photon with energy between E_γ and $E_\gamma+dE_\gamma$ will be Coulomb-scattered such that it leaves the scatterer in the acceptance cone of the analyzer. These electrons will have a distribution in kinetic energy corresponding to their distribution in Compton scattering angle. The number of acceptable electrons with kinetic energy between T and $T+dT$ resulting from photons with energy between E_γ and $E_\gamma+dE_\gamma$ will be given by

$$D(T,E_\gamma)dT=A(\psi,E_\gamma)N\frac{\partial\sigma}{\partial\psi}B(E_\gamma)dE_\gamma\frac{\partial\psi}{\partial T}dT, \tag{4}$$

where $\partial\psi/\partial T$ can be obtained from Eq. (1). To find the total number of acceptable electrons with kinetic energy between T and $T+dT$, we must integrate Eq. (4) over the range of photon energies in the spectrum $B(E_\gamma)$. This will give

$$P(T)dT=N\int A(\psi,E_\gamma)\frac{\partial\sigma}{\partial\psi}B(E_\gamma)\frac{\partial\psi}{\partial T}dTdE_\gamma. \tag{5}$$

Any attempt to evaluate this integral would require explicit use of the relationship between ψ, T, and E_γ. Finally, we have the number of electrons detected when the analyzer is set to detect electrons having a mean kinetic energy T given by

$$n(T)=\int E(T,T')\left[N\int A(\psi,E_\gamma)\frac{\partial\sigma}{\partial\psi}B(E_\gamma)\frac{\partial\psi}{\partial T}dE_\gamma\right]dT', \tag{6}$$

where $E(T,T')$ is the probability of detection of an electron with energy T' when the analyzer is set to detect electrons with mean energy T. The problem now is to find the photon distribution $B(E_\gamma)$ from experimental values of $n(T)$.

It seems reasonable that, for the range of values of T in which we will be interested, $E(T,T')$ will have the same maximum value and the same shape but its characteristic width, ΔT, will depend upon the focusing properties of the magnetic analyzer. We shall assume, therefore, that $E(T,T')$ is unity inside of the interval ΔT centered on T and zero outside of this interval. Furthermore, since the square bracket in Eq. (6) is a slowly varying function of T' and ΔT is small, we can remove it from the integral. Thus

$$n(T)=N\Delta T\int A(\psi,E_\gamma)\frac{\partial\sigma}{\partial\psi}B(E_\gamma)\frac{\partial\psi}{\partial T}dE_\gamma. \tag{7}$$

Now, if we keep $B(E_\gamma)$ constant, the integrand in Eq. (7) is a very sharply peaked function of E_γ. As a first approximation we can remove $B(E_\gamma)$ from the integral, perform the integration numerically, and solve for $B(E_\gamma)$. The result of this approximation is quite good except at very high and very low energies where $B(E_\gamma)$ is changing rapidly. As a second approximation we can make use of the fact that over small energy intervals we know the shape of the spectrum we are measuring. Thus we replace $B(E_\gamma)$ by $B_x(E_{\gamma0})B_s(E_\gamma)/B_s(E_{\gamma0})$, where $B_s(E_{\gamma0})$ is the calculated spectrum and $B_x(E_{\gamma0})$ is the measured value of the spectrum at the energy $E_{\gamma0}$ corresponding to the maximum value of the integrand of Eq. (7) with $B(E_\gamma)$ removed. Equation (7) then becomes

$$n(T)=N\Delta T\frac{B_x(E_{\gamma0})}{B_s(E_{\gamma0})}\int A(\psi,E_\gamma)\frac{\partial\sigma}{\partial\psi}B_s(E_\gamma)\frac{\partial\psi}{\partial T}dE_\gamma. \tag{8}$$

Note that we are making use of the shape of the theoretical spectrum over a very small energy interval but not of its magnitude. We can now solve for the measured

spectrum

$$B_x(E_{\gamma 0})=\frac{n(T)B_s(E_{\gamma 0})}{N\Delta T P_s(T)}, \tag{9}$$

where $P_s(T)$ is the integral in Eq. (8).

In order to use Eq. (9), we must be able to evaluate the quantities ΔT and $P_s(T)$. If monochromatic γ-ray sources with sufficient intensity and with energies covering the desired range of the spectrometer were available, ΔT and $P_s(T)$ could be measured experimentally. This not being the case, we must rely upon a theoretical calculation of these quantities. Such a calculation will depend upon the design of the Compton spectrometer and thus a description of it would seem appropriate at this point.

The principal components of the spectrometer are a scattering chamber in which a narrow beam of x-rays which has been collimated and cleared of charged particles is incident upon a metal scatterer (A in Fig. 1), a deflection chamber in which the electrons leaving the scatterer in a small solid angle are analyzed in a magnetic field (B) and a detecting system (C) for the electrons selected by the analyzer. The deflection chamber may be positioned to accept electrons scattered at various angles with respect to the x-ray beam. However, to simplify the calculation of $P_s(T)$, electrons in the forward direction were analyzed. The deflection chamber fits between the pole faces of a 60° sector magnet. Electrons with a given small range in energy reach the focal point of the magnetic analyzer and are detected by a plastic scintillator and photomultiplier. The voltage pulses from the photomultiplier are amplified and all those above a certain voltage are recorded. Considerable preliminary investigation showed that the number of recorded pulses was insensitive to small changes in photomultiplier supply voltage, amplifier gain or discriminator level. The output of the betatron was monitored by a transmission ion chamber (F) and a current integrator. The current supply to the analyzing magnet was regulated and the magnetic field was continuously monitored by a probe rotating between auxiliary pole faces.

A 60° focusing magnetic analyzer has a finite resolution given by[10]

$$\Delta T=C\frac{T+2mc^2}{T+mc^2}T, \tag{10}$$

where the constant C depends upon the radius of curvature in the magnetic field and the size of the detector. The calculated value of C for our instrument is 0.0166. This value may be inaccurate because of the neglect of small fringing fields but the value of C will not affect relative spectral measurements.

The Klein-Nishina scattering cross section was obtained indirectly from National Bureau of Standards

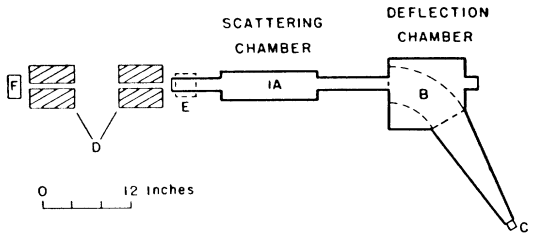

FIG. 1. Schematic diagram of the spectrometer.

Circular 542. The quantity plotted there is the differential cross section per unit electron solid angle, $\partial\sigma/\partial\Omega_\psi$, whereas we want the differential cross section per unit angle. The two are related by

$$\partial\sigma/\partial\psi=2\pi\sin\psi(\partial\sigma/\partial\Omega_\psi). \tag{11}$$

Values of $\partial\psi/\partial T$ were obtained from Eq. (1). The Schiff intensity spectrum in the forward direction for an infinitely thin target with the constant chosen to be 191 was used to obtain $B_s(E_{\gamma 0})$. Katz and Cameron[11] point out that this is actually a good approximation to the intensity spectrum in the forward direction for a thick target in a betatron.

In order to evaluate the function $A(\psi,E_\gamma)$, we must consider the multiple Coulomb scattering of the electrons in the scattering foil. If we assume that the analyzer will accept electrons inside a cone of half-angle α about the direction of the x-ray beam, there will be a certain probability that an electron with kinetic energy T which was Compton scattered at an

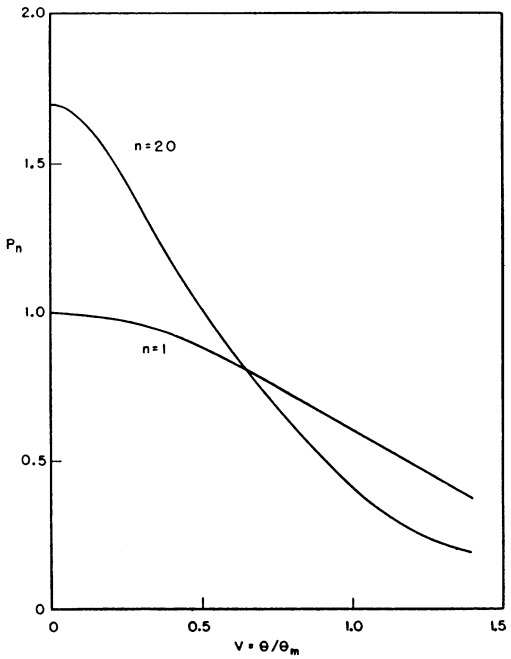

FIG. 2. The Coulomb scattering function P_n.

[10] W. E. Stephens, Phys. Rev. **45**, 513 (1934).

[11] L. Katz and A. G. W. Cameron, Can. J. Phys. **29**, 518 (1951).

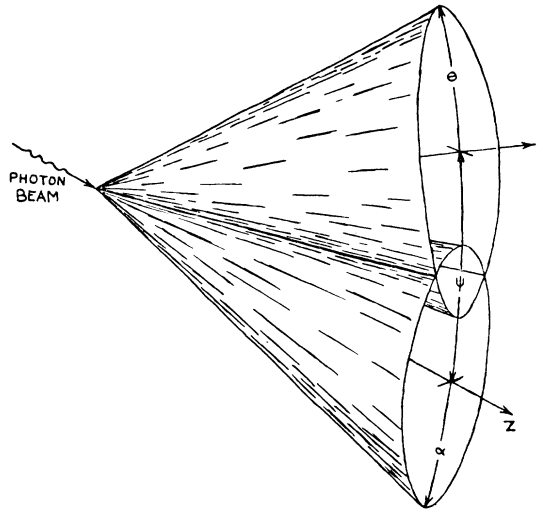

FIG. 3. Schematic representation of Compton scattering followed by Coulomb scattering.

angle ψ with respect to the x-ray beam will, after subsequent Coulomb scattering, be accepted. Since the angle α is small and the scatterer is thin, we may neglect lateral displacements from the axis of the x-ray beam. The probability of multiple scattering of an electron with kinetic energy T through an angle θ in traversing a thickness t of a scatterer with atomic number Z and N electrons per unit volume is given approximately by[12]

$$P(\theta,\theta_m)=\frac{1}{\theta_m}\left(\frac{2}{\pi}\right)^{\frac{1}{2}}\exp\left[-\frac{1}{2}\left(\frac{\theta}{\theta_m}\right)^2\right], \tag{12}$$

where

$$\langle\theta_m\rangle^2=4\pi NtZ^2e^4\frac{(T+mc^2)^2}{T^2(T+2mc^2)^2}\ln\left(\frac{2ap}{\hbar Z^{\frac{1}{3}}}\right), \tag{13}$$

p=momentum of the electron, e=electronic charge, a=Bohr radius, and mc^2=rest energy of the electron. θ_m is called the most probable angle of scattering. Since the Compton electrons originate uniformly throughout the scatterer and thus do not all pass through the entire thickness, Eqs. (12) and (13) do not apply. In order to obtain an appropriate scattering function we consider a scatterer consisting of n slabs of equal thickness y with $1/n$ of the Compton electrons originating at the first surface of each slab. The scattering probability for the electrons from the kth slab will then be

$$P_{n,k}=\frac{1}{\theta_m}\left(\frac{2n}{\pi k}\right)^{\frac{1}{2}}\exp\left[-\frac{1n}{2k}\left(\frac{\theta}{\theta_m}\right)^2\right]. \tag{14}$$

For all n slabs we will have

$$P_n(\theta,\theta_m)=\frac{1}{n\theta_m}\left(\frac{2}{\pi}\right)^{\frac{1}{2}}\sum_{k=1}^{n}\left(\frac{n}{k}\right)^{\frac{1}{2}}\exp\left[-\frac{1}{2}\frac{n}{k}\left(\frac{\theta}{\theta_m}\right)^2\right]. \tag{15}$$

P_n was calculated for five values of n up to $n=20$ and P_{20} was taken to be a good approximation to the actual scattering probability ($n=\infty$). In Fig. 2, P_1 and P_{20} are shown for comparison.

Consideration of Fig. 3 shows that the probability that an electron which has been Compton scattered through an angle ψ and Coulomb scattered through an angle θ will be accepted is equal to the fraction of the surface of a cone with half-angle θ which lies inside a cone with half-angle α; the cones having a common vertex and the angle between their axes being ψ. If we consider the circles which these cones intersect on the surface of a sphere with its center at their common vertex, we see that this probability also equals the fraction of the circumference of the scattering circle which lies inside the acceptance circle. Since only small values of the angles α, ψ, and θ will be used, we may as well draw the circles on a plane. Thus to some convenient scale we can draw a circle with a radius α, and about a point a distance ψ from its center a family of

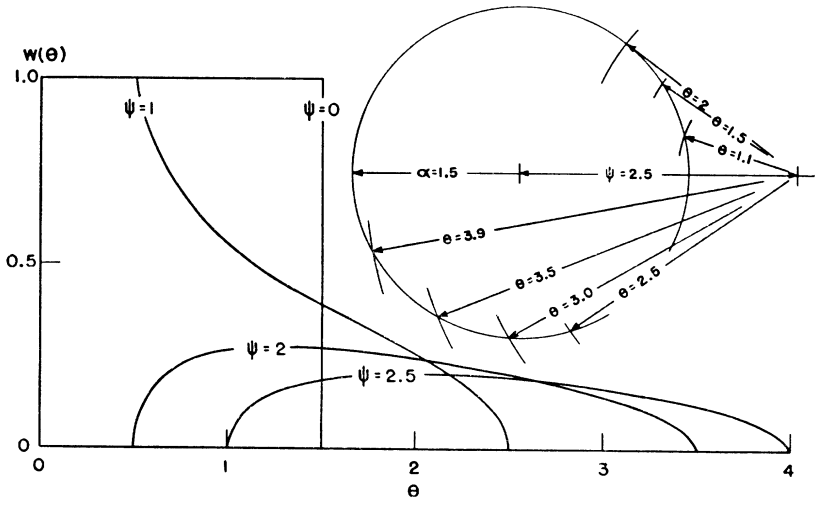

FIG. 4. Graphical construction for $W(\theta,\psi)$ and some representative curves of $W(\theta,\psi)$.

[12] Bethe, Rose, and Smith, Proc. Am. Phil. Soc. **78**, 573 (1938); also see L. H. Lanzl and A. O. Hanson, Phys. Rev. **83**, 959 (1951).

concentric circles with radii θ. The probability of acceptance, $W(\theta,\psi)$, will then be $1/2\pi$ times the angle subtended at the center of the scattering circle by its intersection with the acceptance circle. In Fig. 4, a typical graphical solution for $W(\theta,\psi)$ and some representative curves are shown.

The probability that a Compton electron ejected at an angle ψ with a kinetic energy T will be accepted can now be found from

$$A(\psi,E_\gamma)=\int P_{20}(\theta,\theta_m)W(\theta,\psi)d\theta, \qquad (16)$$

where is it understood that E_γ is a function of ψ and T and that θ_m depends on T and the thickness, atomic number, and electron density of the scatterer. The integral in Eq. (16) was evaluated graphically. A typical curve of the integrand is shown in Fig. 5. All of the factors in the integrand in Eq. (8) are now known and the integral can be evaluated graphically. Two typical curves of the integrand of Eq. (8) are shown in Fig. 6. Since the "efficiency" of the spectrometer is less by a factor of nearly 3 at 15 Mev than at 5 Mev, the curves have been normalized to approximately equal areas. These curves can be considered to be the response curves of the spectrometer when it is accepting electrons with the indicated kinetic energies. All of the factors in Eq. (9) are now known and the spectrometer may be used to measure a continuous x-ray spectrum.

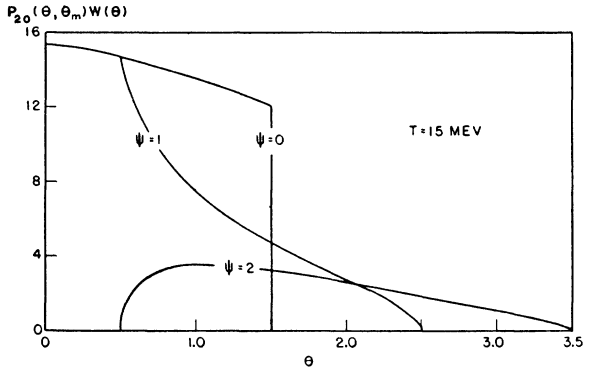

FIG. 5. The integrand in Eq. (16).

In order to understand the behavior of the spectrometer as it depends on energy, we must consider both the Compton effect and Coulomb scattering. At low energies the spread in photon energy which corresponds to Compton electrons in a small cone in the forward direction is small. In the absence of multiple Coulomb scattering, this would lead us to expect the resolution to be best at low energy. However, the chance that Compton electrons from higher energy photons which were initially outside of our small cone can be Coulomb-scattered into the cone is highest at low energies. The combined effect, as can be seen in Fig. 6, is a sharp peak with a long high-energy tail. As the

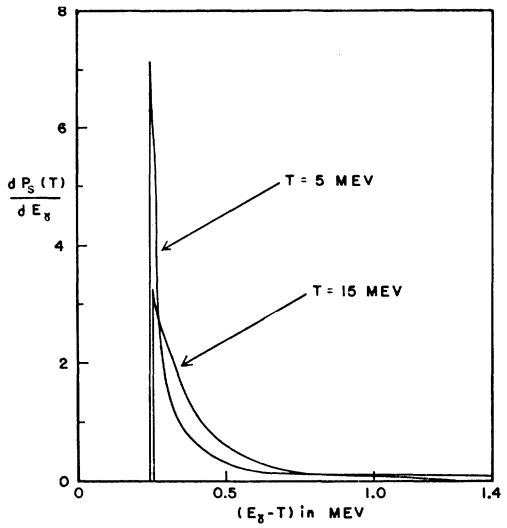

FIG. 6. The integrand in Eq. (8). This is the calculated response of the spectrometer to photons when detecting electrons with kinetic energies of 5 Mev or 15 Mev.

energy of the spectrometer is increased, the percentage spread in photon energy leading to Compton electrons in a small cone in the forward direction increases nearly linearly with the electron's kinetic energy but the chance of Coulomb scattering into the cone becomes less. The 15-Mev curve shows the result to be a much broader peak with a much shorter tail. The seriousness of this for our calculations lies in the angles of scattering which must be considered. The largest scattering angle in the case of the 15-Mev curve was 3.5° while the 5-Mev curve represents scattering angles up to 10°. Because of the rapid increase in the difficulty of the computations in the neighborhood of 5 Mev, this would seem to be a practical lower limit of the use of the type of analysis described here. Owing to the decreasing efficiency of the Compton effect and the increasing competition from pair production, the spectrometer probably has an upper limit of usefulness near 30 Mev.

III. EXPERIMENTAL PROCEDURE

The effect of the magnetic field of the analyzer on the gain of the photomultiplier was thoroughly investigated. It was found that careful orientation of the photomultiplier and the use of a mu-metal shield eliminated any detectable magnetic effect. It was found to be possible to adjust the gain and discriminator level so that essentially all of the pulses due to electrons originating in the scatterer could be observed without the background becoming too large. Under these conditions the data were very insensitive to changes in gain. The over-all gain of the photomultiplier and amplifier and the discriminator level remained constant to within several percent over periods of weeks. This was more than adequate since a measurement at one energy took about two days.

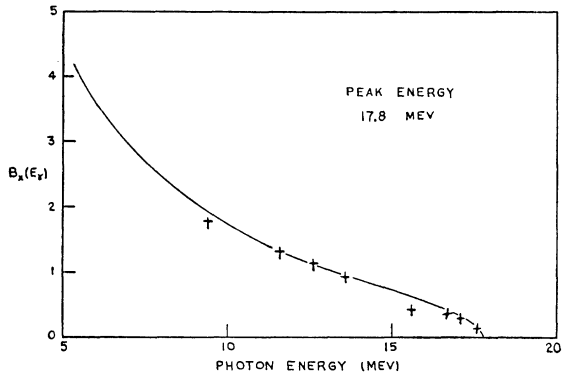

FIG. 7. The result of the spectrum measurement. The solid curve is Schiff's theoretical spectrum.

The determination of each spectrum point required four types of data. The number of Compton and pair electrons was found from the difference between data obtained with the scatterer in and out of the beam. The number of positrons (and presumably of pair electrons) was found from a similar difference with the magnet current reversed. The time devoted to each type of data was determined so as to minimize the total time to get a desired statistical accuracy at a given energy. The data were actually obtained in many short exposures and the deviations from the means were found to be statistically random.

A preliminary energy calibration of the spectrometer was made using the conversion electrons of Cs^{137}. The final calibration involved two steps. The betatron energy scale was determined by comparing C^{12} and $O^{16}(\gamma,n)$ activation curves with similar curves obtained at the University of Saskatchewan.[13] The peak of the measured spectrum was then matched with a calculated spectrum with the correct peak energy. Since the high-energy end of the bremsstrahlung spectrum is very steep, a match here is independent of the assumed spectrometer response. To justify such a one-point calibration, the ratios of the magnetic field at a large number of points in the analyzer field to that at a fixed reference point were measured. These were found to be independent of magnet current up to currents twice as large as any used in this experiment.

The scatterer was a beryllium disk 0.038 in. thick with a diameter of $\frac{5}{8}$ in. At the position of the scatterer the beam had a circular cross section $\frac{3}{8}$ in. in diameter. The scatterer was 63 in. from the betatron target. The radius of curvature of electrons in the magnetic field was 9.25 in. The detector was a cylinder of Plastifluor B $\frac{3}{8}$ in. in diameter and 1.75 in. long. A tungsten target approximately 5 mils thick was used in the betatron. Between the betatron target and the beryllium scatterer the x-ray beam passed through 10 mils of copper (the betatron window) and 15 mils of aluminum (the transmission ion chamber).

[13] L. Katz *et al.*, Phys. Rev. **95**, 464 (1954).

IV. EXPERIMENTAL RESULTS

The results of a measurement of the spectrum of the Case betatron operating at a peak energy of 17.8 Mev are shown in Fig. 7 and in Table I. In order to compare the measurement with theory a choice of the arbitrary vertical scale must be made. This was accomplished by plotting the logarithms of the experimental and theoretical spectra and sliding vertically until the best visual fit was obtained. The sum of the squares of the deviations between theory and experiment weighted by the reciprocals of the standard deviation for each experimental point was compared with similar weighted sums for slightly different choices of vertical scale. The visual fit turned out to be the best fit in this sense. The third column in the table lists the deviation between experiment and theory in units of the standard deviation for each experimental point. It is seen that the deviation is less than one standard deviation for half the data. No correction was made for photons absorbed between the betatron target and the scatterer since less than 1% of even the lowest energy photons suffer this fate.

TABLE I. The results of the spectrum measurement.

$E_{\gamma 0}$ (Mev)	$B_x(E_{\gamma 0})$	δ/σ
9.4	372±11	+0.1
11.6	276±13	+1.1
12.6	237±9	+1.6
13.6	195±9	+0.8
15.6	91±5	−5.8
16.6	75±4	−2.0
17.1	62±4	+0.7
17.6	27±2	−0.5

V. ACKNOWLEDGMENTS

The authors are indebted to the Case betatron crew for their help and particularly to Dr. R. L. Stearns for his assistance in obtaining the experimental data.